Progress In Electromagnetics Research, Vol. 135, 17–35, 2013

HYBRID SIMULATION TECHNIQUE FOR CHARACTERIZING WIRELESS CHANNEL IN MEDICAL ENVIRONMENTS

Priscilla Rong Shu Lee[1] and Viet Phuong Bui[2, *]

[1]Nanyang Technological University (NTU), Nanyang Avenue, Singapore 639798, Singapore

[2]A*STAR Institute of High Performance Computing (IHPC), 1 Fusionopolis Way, #16-16 Connexis, Singapore 138632, Singapore

Abstract—The purpose of this paper is to investigate the use of simulation technology for the analysis of wireless propagation channel in medical environments. In this paper, the channel modeling has been carried out by using an effective simulation platform, which combines full-wave Method of Moments and adaptive ray tracing technique. Base on this, the channel characteristics involving both large-scale and small-scale parameters of a wireless network deployed within a hospital environment can be estimated. Also, it is straightforward to predict the levels of electromagnetic field interference produced from the network infrastructure. The simulated results of four scenarios of medical environment, such as the patient room, the operating room, a particular level of the hospital, and the cardiac stress test room, with different wireless technologies used show the advantage and capability of the presented simulation approach.

1. INTRODUCTION

Advance in wireless communications and miniaturization of electronic devices have made available for the deployment of various wireless systems (e.g., sensor, communications...) in medical environments. This has a great potential to improve efficiency and convenience for both patients and healthcare providers. Indeed, the wireless technologies can contribute towards helping with both access and cost saving, which are two of the main issues in the medical field (e.g., real-time access to patient data, lab results..., communicating

Received 21 October 2012, Accepted 5 December 2012, Scheduled 10 December 2012

* Corresponding author: Viet Phuong Bui (buivp@ihpc.a-star.edu.sg).

the remote patient's status in real-time to caregivers, access to the expensive and large machines from anywhere in the hospital through wireless interface for rapid and flexible deployment, and etc.) [1–3]. It has been seen that current and potential applications of the wireless technologies in the medical field are ubiquitous. ZigBee, Bluetooth technologies are generally used for applications that can tolerate a low transmission rate, but demand long battery life in a Wireless Body Area Network (WBAN) to collect vital health information such as Electrocardiogram (ECG), blood pressure... GPRS/UMTS wireless communication system is deployed to monitor patients in critical conditions inside hospitals or in remote areas. Ultra Wide Band (UWB)-based video transmission system is used in the operating room to provide a reliable connection, high quality images, and safety radiation level. Patient data transfer around the hospital and communication between multiple medical devices within the hospital is made possible through Wireless Local Area Network (WLAN) channels. The short-range 60 GHz radio technology may help enhancing privacy and data protection. RFID technology is used in hospitals to keep track of equipment or patients to know their whereabouts as well as monitoring hospital supply stocks in real-time. As a result, commercial sectors rapidly thrive with lots of applications such as CodeBlue project, MobiHealth Body Area Network System, LifeSync Wireless Electrocardiogram System, and HealthTrax RFID Asset Tracking Software, just to name a few [4–6].

The challenges that are faced when deploying wireless networks in the medical field include several factors, such as different wireless devices working at different frequencies, strict guarantees needed because patients well-being may depend on it, different behavior of wireless devices at different times and locations due to natural and unnatural issues. Also, implementing medical devices using wireless technology requires information need to be effectively transmitted from the source device to the targeting device in different scenarios of medical environment [7–11]. Hence, in order to optimize the design and performance of such a wireless system, a proper channel propagation modeling is needed. In addition, the channel design has a need to limit the transmission power in order to ensure no Electro-Magnetic field Interference (EMI) occurred between deployed wireless system and critical medical devices coexisted in the environment.

Many research works have been carried out to investigate the characteristics of wireless channel in the area of medical applications by using measurement techniques [12–16]. Otherwise, the simulation technology is attractive because it is far less costly compared to the long, labor-intensive measurement campaigns, and it is easily adapts

for different environment setups. However, channel analysis in the presence of a multipath propagation is a challenging task due to the "electrically" large size of the computational domain involved. It can be seen that the difficulties for modeling are due to the multi-frequency band and multi-scale of the whole environment. The devices used for different purposes can cover a wide frequency spectrum, and the overall dimension of the confined environment is extremely huge (on the order of thousands of wavelengths) in comparison with the small devices used inside. Hence, solving the entire Electro-Magnetic (EM) propagation problem using full-wave numerical methods such as Method of Moments (MoM), which requires a discretization of the computational domain, are impractical due to the enormous memory requirements. On the other hand, oversimplifying the geometry to make it amenable to the Uniform Theory of Diffraction (UTD) simulation might severely compromise the modeling accuracy [17]. Therefore, this paper presents a hybrid simulation platform, which combines full-wave MoM and UTD/adaptive ray tracing technique for wireless channel modeling in a medical environment. Key channel parameters such as pathloss, RMS delay spread, and local fading statistics of the received signals can be extracted. The simulations will be performed in four different scenarios of medical environments, i.e., patient room, operation room, a particular level of the hospital, and cardiac stress test room.

2. MODELING OF WIRELESS PROPAGATION CHANNEL

A scenario of medical environment includes a room or several rooms with separated thin walls in which lots of objects are located (bed,

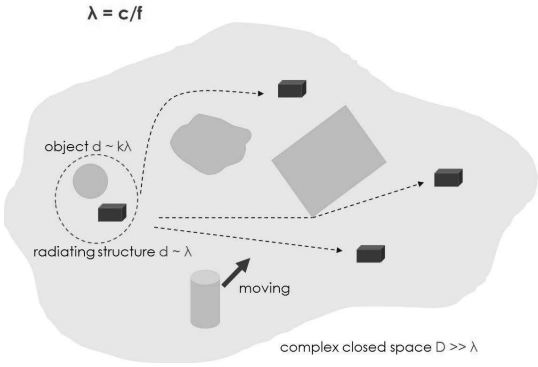

Figure 1. Medical environment with multiple & moving objects.

table, chair, medical machine device etc.). To deploy a wireless system, a transmitter is needed to send a signal out at the transmitter location, and a receiver is needed to receive and detect the signal at the receiver location. In such a problem, the overall problem domain is electrically very large, but involves structures with many details (antenna, small objects etc.) as depicted in Figure 1, that cannot be ignored in the modeling. Therefore, to solve this multi-scale EM problem, one can break up the problem domain into a number of smaller manageable sub-domains and solve each sub-domain separately [18].

2.1. Hybrid Simulation Technique

In the hybrid scheme, the MoM is first utilized to model the transmitting/receiving antennas (Tx/Rx) and their nearby objects. The results obtained from the MoM solution, i.e., antenna working parameters, such as input impedance, gain etc., are taken as the equivalent sources and will be substituted into the UTD/ray tracing-based simulation, which calculates the long distance coupling between each pair of transmitter and receiver.

According to the UTD, the mechanisms of wave propagation can be distinguished as direct radiation, reflection, diffraction, and their combinations with each of them being represented by a ray. The rays arrive at the receiving locations via different paths, resulting in the so-called multipath problem. A 3D image-based ray tracing technique is first used to determine the propagation paths. The UTD is then utilized to calculate the fields associated with the rays. The whole environment is discretised by using planar polygonal facet. Each facet is associated with the electromagnetic properties such as relative dielectric constant, electrical conductivity, and thickness which are relevant for EM field calculations. The Binary Space Partitioning-based acceleration algorithm is needed to deal with numerous shadowing judgments for each ray path [19–21]. The antenna's locations should be a distance away from walls (at least multiple wavelengths apart) for ray tracing to be effective. If this were not the case, a technique based on combining the Integral Equation (IE) method with the Multiple Image Theory (MIT) is proposed [22]. In enclosed spaces, the direct rays and multi-reflected rays contribute more to the couplings than the diffracted rays. This is different from the open space, where the diffracted rays are the major contribution in the shadow region. Hence, an adaptive technique for ray tracing simulation in different environments must be developed.

Once the propagation paths are determined, the UTD expressions can be applied to calculate the field values for each ray [19, 23]:

- Direct field $\{\mathbf{E}_I\}$;
- Transmitted, reflected field $\{\mathbf{E}_T,\ \mathbf{E}_R\}$ created by a facet; the transmission and reflection coefficients for the soft and hard field components are computed in the local ray-fixed coordinate system;
- Diffracted field $\{\mathbf{E}_D\}$ generated by an edge/wedge; the modified diffraction coefficients (finite conductivity) for the soft and hard field components are obtained based on the edge-fixed coordinate system.

The electric field and received power can be combined coherently at the receiving points:

$$\vec{E}_r = \sum_{i=1}^{N} \vec{E}_i, \quad P_r = \sum_{i=1}^{N} P_i, \tag{1}$$

where N is the number of propagation paths; $\vec{E}_i$ and P_i are the complex electric field and time-averaged power of the ith path, respectively. Hence, the EMI field at a typical location is determined by vectorially summing the EM field levels of all the multipath rays that intersected that location. The time of arrival, direction of arrival/departure for each propagation path etc., which can be used to extract the parameters of the radio channel, are also provided.

2.2. Wireless Channel Modeling

The radio channel is characterized by three key parameters that largely represent its response for both narrow and wide bandwidths: pathloss, local fading distribution of the received signals, and RMS delay spread. These parameters are useful in describing the overall characteristics of the multipath profile and are essential in developing design guidelines for a wireless system [24–26]. The large-scale pathloss, which is the value of the transmit power divided by the locally averaged received power, is given by:

$$PL\,(\mathrm{dB}) = P_t\,(\mathrm{dBm}) - P_r\,(\mathrm{dBm}) - L_S\,(\mathrm{dB}), \tag{2}$$

where L_S is the sum of all other losses in the system (e.g., cable loss). A commonly used large scale model is the log-distance pathloss model with log normal shadowing can be described as:

$$PL(d) = PL_{FS}(d_0) + 10n\log_{10}(d/d_0) + X_S, \tag{3}$$

where $PL(d)$ is the average pathloss value at Tx-Rx separation distance d, $PL_{FS}(d_0)$ is the pathloss at a reference distance d_0, and n is the pathloss exponent; X_s is the shadowing term that has normal distribution with zero mean.

The time invariant impulse response $h(t)$ is described as the sum of N multipath components having random amplitudes a_k, delay τ_k and phase θ_k:

$$h(t) = \sum_{k=1}^{N} a_k \delta(t - \tau_k) e^{j\theta_k}, \tag{4}$$

where δ is the Dirac delta function. The RMS delay spread τ_{rms} is then extracted as given by:

$$\tau_{rms} = \left(\sum_k \left\{ (\tau_k - \tau_m - \tau_1)^2 a_k^2 \right\} \Big/ \sum_k a_k^2 \right)^{1/2}, \tag{5}$$

where τ_m is the mean excess delay and τ_1 the first delay

$$\tau_m = \sum_k \left\{ (\tau_k - \tau_1) a_k^2 \right\} \Big/ \sum_k a_k^2. \tag{6}$$

The received signal is a random variable respect to position. Hence, the probability distribution characteristics, e.g., Rician, Nakagami..., could be used to describe its local fading statistics. The theoretical parameters can be estimated based on the moment method or

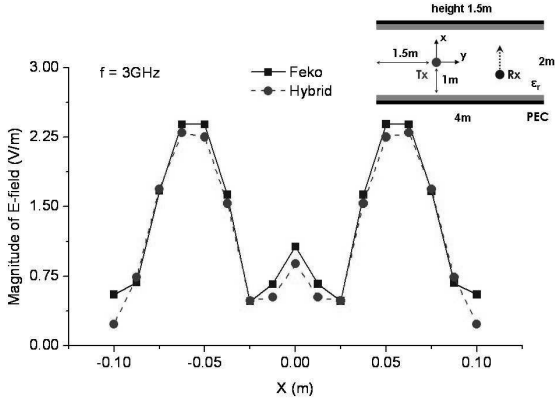

Figure 2. Comparison between our hybrid simulation and Feko software — Electric field distributed along X direction at the receiving points $(x_r,\ y_r,\ z_r) = (X,\ 1.5,\ 0.0)$. Transmitting antenna is located at the origin of the coordinate system. The dimensions of the corridor are $2 \times 4 \times 1.5$. The structure is geometrically symmetric with respect to the XY and YZ planes. All dimensions are in meter. The corridor is made by PEC-backed coating wall with $\varepsilon_r = 4$, $\sigma = 0.01\,\mathrm{S/m}$, and coating thickness $d = 0.005\,\mathrm{m}$.

Table 1. Comparison of memory requirements and CPU time — Corridor model.

Technique	Memory requirements [MB]	CPU time [sec]
MLFMM (Feko)	4000	1800
Hybrid	10	150

Maximum-Likelihood Estimation (MLE). A Kolmogorov-Smirnov test is generally used to decide the goodness-of-fit of the observation data to the theoretical distribution.

3. SIMULATION RESULTS

Figure 2 shows a model that consists of a corridor-like structure and a transmitting antenna. This vertically polarized disc-cone operates at single frequency of 3 GHz, although it also allows operation over a range of frequencies. For verification purpose, the Multilevel Fast Multipole Method (MLFMM) full-wave EM simulator — Feko is employed to simulate this electrically large structure. The levels of EM fields within the corridor are then investigated. Figure 2 demonstrates a good agreement between our hybrid model (denoted as Hybrid) and Feko. Table 1 illustrates that our technique requires much less CPU time and memory. Some discrepancies appear nearby the walls, which are caused by near-field effect.

A larger model representing a corridor with dimensions of 1.62 m width, 10.6 m length, and 4.5 m height, is simulated. The first scenario consists of two disc-cone antennas used as the Tx and Rx. The power intensity is determined when the Rx is moving along the corridor. The simulation of such electrically large structure is a big challenge, even for the MLFMM which is mainly due to limited resources of computer memory. The measurement was then conducted in a building corridor as shown in Figure 3. The received power is captured and then compared with simulated results based on our hybrid model. We notice that two curves follow the same trend, except at some locations because of the uncertainties such as environment, location and so on. Rapid fluctuations of the received signal can be seen at some receiving points. The second scenario includes two fixed transmitting antennas simultaneously operating and a mobile receiving antenna as depicted in Figure 3. In this case, the interference is detected at the Rx, especially mid-way between the two transmitting antennas. The power is increased by about 5 dBm$\sim$8 dBm. A good correlation can be observed as the simulated results mostly lie in the range of the

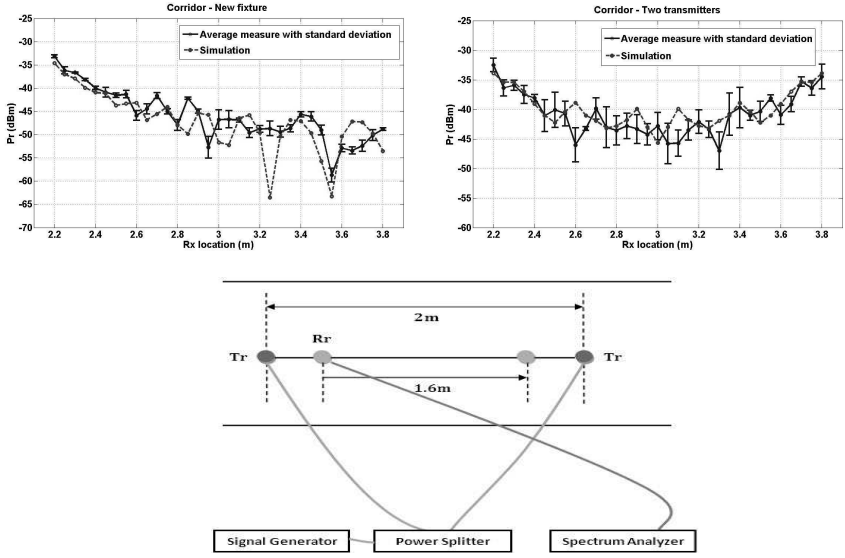

Figure 3. Comparison between the simulated and the measured results (first and second scenario) — Measurement layout — Disc-cones operating at centre frequency of 3 GHz (frequency span 400 MHz). The power of 5 dBm is transmitted from signal generator/power splitter. The corridor includes right concrete wall ($\varepsilon_r = 4.0$, $\sigma = 0.01\,\mathrm{S/m}$, $d = 0.2\,\mathrm{m}$), left wood wall ($\varepsilon_r = 3.0$, $\sigma = 0.005\,\mathrm{S/m}$, $d = 0.1\,\mathrm{m}$), and concrete floor ($\varepsilon_r = 4.0$, $\sigma = 0.01\,\mathrm{S/m}$, $d = 0.2\,\mathrm{m}$). 2D cut-plane shows locations of Tx and Rx above the floor at the same height of 1 m. Measurements repeated with all equipment dismantled and re-calibrated; the measured results are quite reliable and repetitive.

measured values.

The simulations of radio propagation in medical environments such as patient room, operation room, a particular level of the hospital and cardiac stress test room were performed. We extracted the key channel parameters such as large-scale pathloss, time delay spread and local distribution of the received signals that can be used to analyze and optimize the channel performance. In all simulations, the transmitter's location is selected to best suit the actual environment. To accurately predict the rapid fluctuations of the received signals, the distance between two observations should be smaller than $\lambda/4$ where λ is the wavelength. In large-scale simulations, a rectangular grid of receivers with a spacing of at least 2λ needs to be established. The material properties of the medical environments are given in Table 2.

Table 2. Material properties of the simulated medical environments.

Material	Relative permittivity ε_r	Conductivity σ (S/m)	Thickness d (cm)
Concrete	5	0.04	10
Wood	2.3	0.04	5
Glass	6	0.005	0.2
Plastic	4.25	0.013	5
Body tissue	38.568	1.27	50
Metallic object	1	10000	0.1
Metallic wall	1	1000	0.1

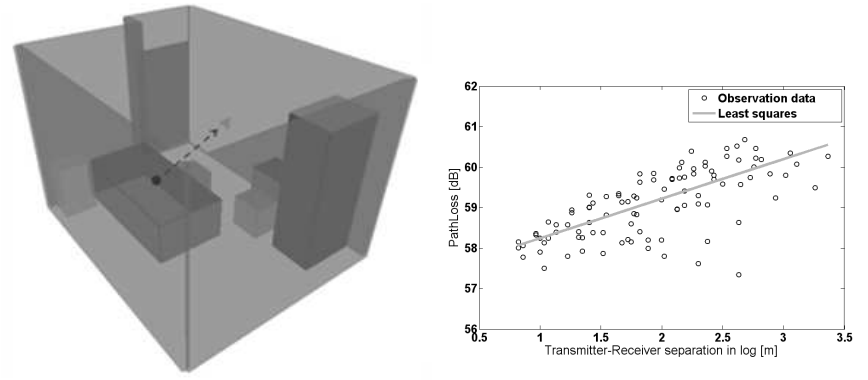

(a) (b)

Figure 4. (a) Description of a patient's room; its dimensions are 3 m × 4 m × 2.5 m; Tx is near the bed area; Rx is mounted near the ceiling in the middle of the room. (b) Log normal distribution-based pathloss model inside the room.

3.1. Patient Room

The geometrical model consists of typical furniture such as bed, cupboard, chair and table, located in the patient room as depicted in Figure 4(a). The monitoring application is of particular interest in this scenario where a patient carrying a sensor BAN transmits data to a fixed receiver by using wireless technologies such as Bluetooth or Zigbee. The information obtained from the sensors attached to patient's bodies is transmitted via a network Access Point (AP) to the nursing room. Hence, nurses are able to monitor patients in real-

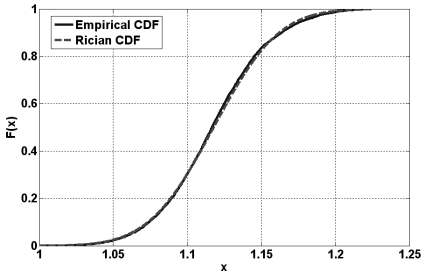

Figure 5. Fading statistics of the normalized received power.

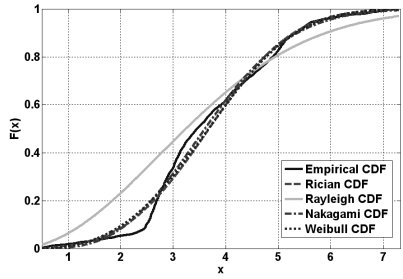

Figure 6. Local distribution of delay spread of the received signals.

time without having to visit them frequently. This saves them time and gives them the opportunity to take care of more patients within the hospital. The half-wavelength wire antennas, which operate at the frequency of 2.45 GHz, represent emitting and receiving devices. The transmit power is 5 mW. The receiving nodes are placed at different locations inside the patient room.

As shown in Figure 4(b), the pathloss model follows a log normal distribution with pathloss exponent $n = 1.0$. The signal strength gradually attenuates with the distance from the transmitter to the receiver as there is no obstruction of the EM wave.

The received signal is fluctuated in the patient room due to the effect of multipath propagation. Figure 5 indicates the empirical Cumulative Distribution Function (CDF) of the normalized received power inside the room. It can be seen that the Rician distribution best fits the received signal data as this satisfies Kolmogorov-Smirnov criterion. In this environment, the propagation is dominated by the direct path as there is line-of-sight between the transmitter and the receiver. Figure 6 shows the empirical CDF of the local distribution of delay spread of the received signals inside the patient room. We found that the theoretical Rician distribution minimizes the Kolmogorov-Smirnov criterion. The estimated parameters are listed in Table 3.

3.2. Operation Room

Considered as one of the most complex areas of the hospital, the operation room largely differs to the patient room, as shown in Figure 7. The wall is made of metal for EM shielding instead of typical concrete wall. The geometrical model consists of metallic beds, tables and partition walls. In this scenario, the high-speed UWB

Table 3. Estimated parameters for local distribution of delay spread.

Distribution	Patient room	Operation room	Cardiac stress test room	Particular level of the hospital
Rayleigh	$\sigma = 2.76$	$\sigma = 12.12$	$\sigma = 2.94$	-
Rician	$\upsilon = 3.44$ $\sigma = 1.30$	$\upsilon = 11.01$ $\sigma = 9.29$	$\upsilon = 3.73$ $\sigma = 1.30$	$\upsilon = 0.31$ $\sigma = 3.72$
Nakagami	$\mu = 2.23$ $\Omega = 15.19$	$\mu = 1.09$ $\Omega = 293.80$	$\mu = 2.48$ $\Omega = 17.32$	$\mu = 0.65$ $\Omega = 27.70$
Weibull	$a = 4.12$ $b = 3.21$	$a = 17.39$ $b = 2.16$	$a = 4.41$ $b = 3.54$	$a = 4.90$ $b = 1.53$

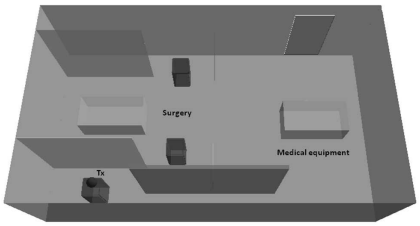

Figure 7. Description of the operation room with dimensions of 10 m × 5.8 m × 2.8 m.

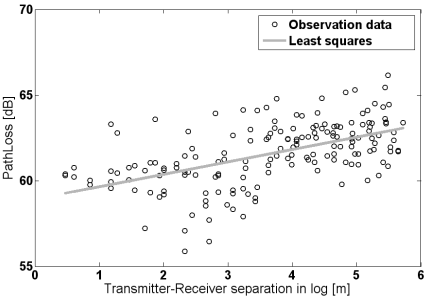

Figure 8. The line corresponds to the linear regression fit for the pathloss model.

radio technology, which has robust performance in dense multipath environment, would be deployed for video transmission between devices used in the operation room. The simulations are performed at the operating frequency of 3.1 GHz. The transmitting device, i.e., disc-cone antenna, which is positioned at the desk level, 1.15 m above the floor, transmits the radiated power of 17 mW. The received signals are observed around the surgery area.

It can be seen that multi-reflections are the predominant paths in the operation room due to metallic walls and internal objects. Hence, after several reflections on the walls, the EM wave still can transfer a significant amount of energy to the receiver. The received signal strength is thus less attenuated as compared to other environments. We observed a slow increase of the pathloss with increase of the transmitter-receiver separation as depicted in Figure 8. The log-

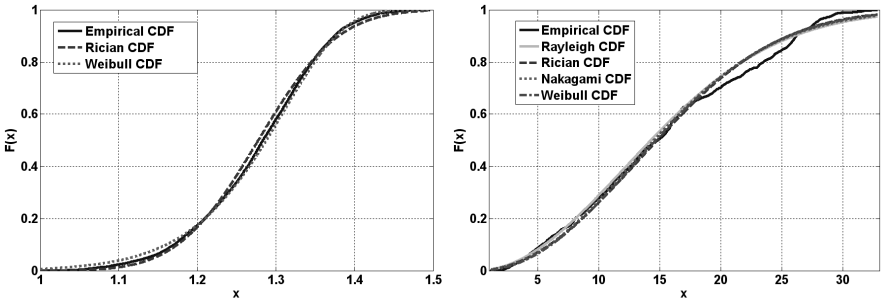

(a) (b)

Figure 9. (a) Fading statistics of the received signals inside the operation room. (b) Local distribution of delay spread of the received signals.

distance pathloss model, which has pathloss exponent $n = 0.75$ and standard derivation of 1.4, provides a good match for the pathloss distribution.

In such a confined space, a large number of signals that occur from the metallic walls and obstacles produce strong multipath effects. As a result, when the receiver moves locally, rapid fluctuations of the received signal strength cause severe fading. The channel design thus becomes more complicated. Figure 9(a) provides the empirical CDF of local distribution of the received signals and an estimation of their fading statistics within the operation room. The Weibull distribution, which minimizes the Kolmogorov-Smirnov criterion, provides a better match for the statistics of fading. In the operation room, we noticed that the signal takes longer path before reaching the receiver resulting in more delay components. The empirical CDF of local distribution of delay spread of the received signals is depicted in Figure 9(b). Again, Kolmogorov-Smirnov test is used to determine which distribution best fits the simulated data. The distribution which minimizes the Kolmogorov-Smirnov criterion is the Rayleigh distribution. Table 3 provides a list of estimated parameters.

3.3. Cardiac Stress Test Room

The scenario of a cardiac stress test room in which a patient is running on the cardio machine is depicted in Figure 10(a). Stress ECG is an essential diagnostic tool that measures and records electrical activity of the heart. The heart information can be recorded by using a sensor attached in front of the chest of the patient. Instead of using the

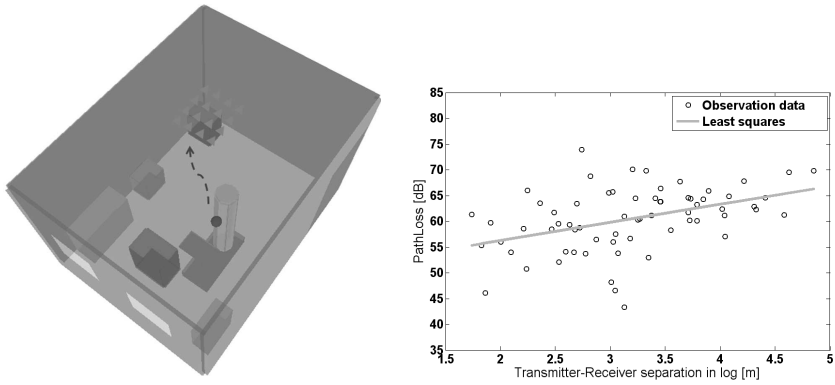

(a) (b)

Figure 10. (a) Room layout for cardiac stress testing (4 m × 3 m × 2.5 m). (b) Pathloss distribution in the cardiac stress test room when the separation distance between the transmitter and receiver increases.

wires to transfer the information from the sensor to the computer located inside the room, a wireless connection can be set up for data transmission. This eventually enables new degree of patient mobility over a wire system. Additionally, the safety is increased by removing a possible danger and point-of-failure (i.e., the wires). As a result, patient safety and hospital productivity have been improved. In this environment, Bluetooth technology would be deployed to collect and emit the patient data. A vertically polarized half-wavelength wire antenna, which is in close proximity to the body's chest at a distance of 1 cm, is used to radiate the power of 5 mW at the operating frequency of 2.45 GHz.

A lossy homogeneous dielectric cylinder of 0.05 m radius and 1.7 m height commonly used as a quasi-human body model in the EM analysis was constructed to represent the patient. The effective constitutive parameters of the body tissues are taken into account in the simulations [27]. It should be noted that the presence of the human body heavily distorts the antenna pattern regardless of the application. The behaviour of EM wave propagation is remarkably affected due to the absorption of the body tissues, causing loss of signal strength. Figure 10(b) shows that the pathloss model, which follows a log normal distribution with pathloss exponent $n = 3.5$ and standard derivation of 3.614, provides a best fit for the pathloss distribution.

The received signals are entirely weak around the receiver location due to the fact that the human body absorbs a portion of emitted power. In this case, the fast fading is not quite severe. Figure 11

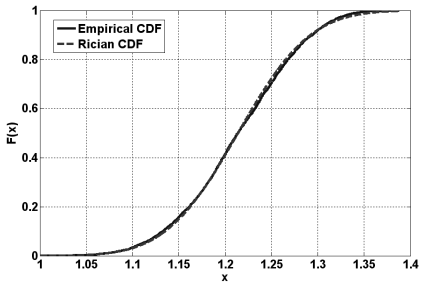

Figure 11. Estimation of fading statistics of the received signals.

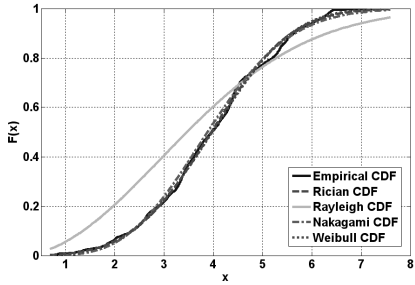

Figure 12. Local distribution of delay spread of the received signals.

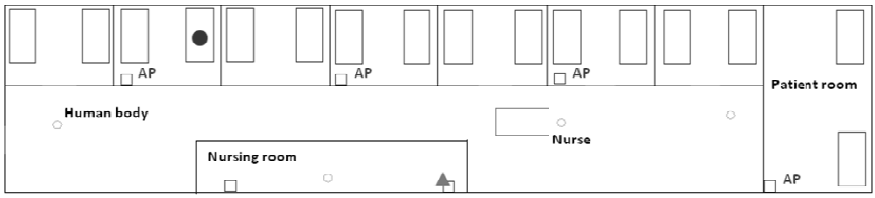

Figure 13. Layout of a particular level of the hospital (32 m × 7 m × 2.5 m).

shows the empirical CDF of the received signals within the cardiac stress test room. The Rician distribution is a good fit to the simulated observations according to Kolmogorov-Smirnov criterion. The empirical CDF of local distribution of delay spread of the received signals and different fitted theoretical distributions are provided in Figure 12. It has been seen that Weibull CDF, which minimizes the Kolmogorov-Smirnov (KS) criterion, best fits the observation data. Table 3 lists a summary of the estimated parameters.

3.4. Particular Level of the Hospital

Figure 13 represents a particular level of the hospital where a WLAN is deployed for transferring data as well as providing a continuous monitoring. It should be noted that multiple overlapping access points can fully cover the area of interest. This system allows doctors to measure vital signs and collect other medical information from the patients remotely, also allows patients to be fully mobile whilst undergoing health monitoring. In this environment, there is a wide

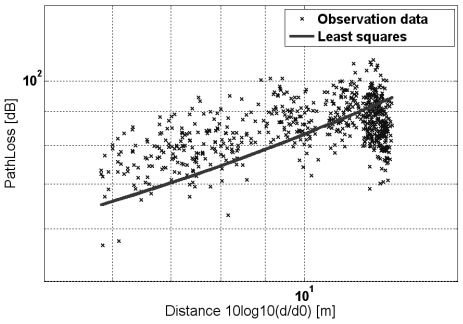

Figure 14. Pathloss distribution — Both axes are in logarithmic scale.

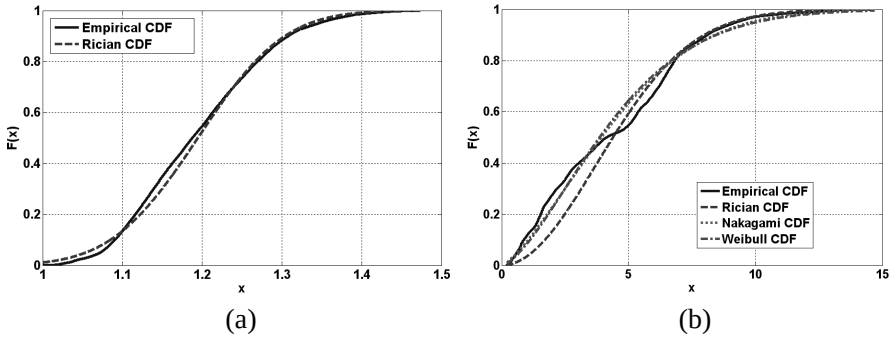

Figure 15. (a) Statistics of fading of the received signals. (b) Local distribution of delay spread of the received signals.

variety of partitions, obstacles as well as the movement of the human bodies. A vertically polarized half-wavelength wire antenna, which locates near the ceiling in the nursing room, 2.2 m above the floor, transmits the power of 5 mW at the operating frequency of 2.45 GHz.

The EM wave experiences many interactions, i.e., through different propagation mechanisms, with walls and obstacles as well as the obstruction by the human bodies, resulting in large transmission loss. Figure 14 shows a sharp increase of the pathloss with increasing transmitter-receiver separation. Again, the log-distance pathloss model indicates a best match for the pathloss distribution with pathloss exponent $n = 4.5$ and standard derivation of 5.5. In such an environment, strong multipath and shadowing effects lead to channel fading. This may results in signal distortion being difficult to detect by the receiver. The cumulative probability for received signals is shown

in Figure 15(a). It has been seen that the Rician distribution best fits the empirical CDF according to the Kolmogorov-Smirnov criterion.

The EM wave eventually travels longer before reaching the receiver because of the large size of the environment. Figure 15(b) provides the empirical CDF of local distribution of delay spread of the received signals. A Kolmogorov-Smirnov test is used to decide the goodness-of-fit of the empirical data. It has been found that Nakagami distribution fitted most of the data sets with a minimum significance level. A summary of parameters of the theoretical distributions estimated by using the method of MLE is given in Table 3.

4. CONCLUSION

Due to the accessibility and mobility requirements, wireless is the preferred medium in medical applications. Besides bringing more comfort and better service to patients, there are large benefits in reducing costs for hospital. Unlike traditional indoor wireless systems, it is crucial to ensure robustness of the radio channel in medical environment as well as no electromagnetic interference to the hospital equipments as the patients' lives are at stakes. This paper explores the use of simulation technology for the characterization of wireless propagation channel in medical environments. A hybrid simulation platform, which combines full-wave MoM and UTD/adaptive ray tracing technique, is proposed to model the radio channel of a wireless network deployed in medical fields, also predict the levels of EM interference produced from the network infrastructure. The analysis of propagation channel in four different scenarios of hospital environment such as patient room, operation room, a particular level of the hospital and cardiac stress test room with different wireless technologies has been performed. Three key channel parameters that can be used to optimise the design of a wireless system are extracted for each environment — large-scale pathloss, time delay spread, and local distribution of the received signals.

The geometrical structure and material properties have great impact on the EM wave propagation. Simulated results demonstrate that different materials and geometrical structures lead to large variation of received signals. Different channel characteristics are observed in the considered medical environments. The radio channel experiences significant loss inside a particular level of the hospital because of a wide variety of partitions, obstacles, and obstructions of the human body. Though the pathloss is less important in the patient room, the sensor BAN may face severe interference problem in the presence of 802.11 networks. The fading is significant inside the

operation room due to metallic wall and scatterers. Otherwise, it were not the case in the cardiac stress test room because the human body absorbs so much energy. However, ECG sensor must be designed to deliver a signal of sufficient power for good reception by the targeted terminal while keeping the radiated power below levels that can create a health hazard. It can be seen that the theoretical Rician distribution, which has been widely used in wireless communications, best fits the received signal data, except in the operation room where the Weibull distribution provides a better match for fading statistics of the received signals. The local distribution of delay spread of the received signals inside the patient room follows Rician distribution. In the operation room, the distribution, which minimizes the Kolmogorov-Smirnov criterion, is the Rayleigh distribution. It has been found that Weibull CDF provides a best match in the cardiac stress test room, while Nakagami distribution fitted most of the data sets with a minimum significance level in a particular level of the hospital. The findings will help engineers in the design of a robust wireless channel in medical environments, also in the assessment of potential risks to hospital equipments.

REFERENCES

1. Chevrollier, N. and N. Golmie, "On the use of wireless network technologies in healthcare environments," *Proceedings of the 5th IEEE Workshop on Applications and Services in Wireless Networks (ASWN2005)*, 147–152, Paris, France, Jun. 2005.
2. Chu, Y. and A. Ganz, "A mobile teletrauma system using 3G networks," *IEEE Transactions on Information Technology in Biomedicine*, Vol. 8, No. 4, 456–462, Dec. 2004.
3. Shnayder, V., et al., "Sensor networks for medical care," Harvard University Technical Report TR-08-05, Apr. 2005.
4. Soomro, A. and D. Cavalcanti, "Opportunities and challenges in using WPAN and WLAN technologies in medical environments," *IEEE Communications Magazine*, Feb. 2007.
5. Kyrö, M., et al., "Measurement based path loss and delay spread modeling in hospital environments at 60 GHz," *IEEE Transactions on Wireless Communications*, Vol. 10, No. 8, Aug. 2011.
6. Noorzaie, I., "Survey Paper: Medical applications of wireless networks," http://www.cse.wustl.edu/∼jain/cse574-06/medical_wireless.htm.
7. Hara, S., et al., "A receiver diversity technique for ensuring high reliability of wireless vital data gathering in hospital rooms,"

Proceedings of the 32nd Annual International Conf. of the IEEE Engineering in Medicine and Biology Society (EMBC), Buenos Aires, Argentina, Aug. 31–Sep. 4, 2010.

8. Scanlon, W. G., "Analysis of tissue-coupled antennas for UHF intra-body communications," *Proceedings of the 12th IEEE Intl. Conf. Antennas & Propagation*, Vol. 2, 747–750, Apr. 2003.
9. Osman, M. A. R., M. K. Abd Rahim, N. A. Samsuri, H. A. M. Salim, and M. F. Ali, "Embroidered fully textile wearable antenna for medical monitoring applications," *Progress In Electromagnetics Research*, Vol. 117, 321–337, 2011.
10. De Francisco, R., L. Huang, and G. Dolmans, "Coexistence of WBAN and WLAN in medical environments," *Proceedings of the 70th IEEE Vehicular Technology Conference*, Anchorage, AL, USA, Sep. 20–23, 2009.
11. Hou, J., B. Chang, D.-K. Cho, and M. Gerla, "Minimizing 802.11 interference on Zigbee medical sensors," *Proceedings of the 4th International Conference on Body Area Networks (Bodynets2009)*, Los Angeles, CA, USA, Apr. 1–3, 2009.
12. Golmie, N., D. Cypher, and O. Rebala, "Performance analysis of low rate wireless technologies for medical applications," *Computer Communications*, Vol. 28, No. 10, 1255–1275, Jun. 2005.
13. Huang, L., R. de Francisco, and G. Dolmans, "Channel measurement and modeling in medical environments," *Proceedings of the 3rd International Symposium on Medical Information and Communication Technology, (ISMICT2009)*, Montreal, Canada, February 24–26, 2009.
14. Mahfouz, M. R. and M. J. Kuhn, "UWB channel measurements and modeling for positioning and communications systems in the operating room," *Proceedings of the IEEE Topical Conference on Biomedical Wireless Technologies, Networks, and Sensing Systems (BioWireleSS2011)*, Phoenix, USA, Jan. 16–20, 2011.
15. Monti, G., L. Tarricone, and C. Trane, "Experimental characterization of a 434 MHz wireless energy link for medical applications," *Progress In Electromagnetics Research C*, Vol. 30, 53–64, 2012.
16. De Francisco, R., "Indoor channel measurements and models at 2.4 GHz in a hospital," *Proceedings of the IEEE Global Telecommunications Conference — GLOBECOM2010*, Miami, FL, USA, Dec. 6–10, 2010.
17. Sahalos, J. N. and G. A. Thiele, "On the application of the GTD-MM technique and its limitations," *IEEE Transactions on Antennas and Propagation*, Vol. 29, 780–786, Sep. 1981.

18. Medgyesi-Mitschang, L. N. and D.-S. Wang, "Hybrid methods in computational electromagnetics: A review," *Computer Physics Communications*, Vol. 68, 76–94, 1991.
19. Cátedra, M. F. and J. Pérez, *Cell Planning for Wireless Communications*, Artech House, Reading, MA, 1999.
20. Haarscher, A., P. De Doncker, and D. Lautru, "Uncertainty propagation and sensitivity analysis in ray-tracing simulations," *Progress In Electromagnetics Research M*, Vol. 21, 149–161, 2011.
21. Kim, H. and H. Lee, "Accelerated three dimensional ray tracing techniques using ray frustums for wireless propagation models," *Progress In Electromagnetics Research*, Vol. 96, 21–36, 2009.
22. Zhao, W. J., E. P. Li, V. P. Bui, and B. F. Wang, "Modeling of transmission characterisation in aircraft cabins with a hybrid technique," *Proceedings of the 2011 IEEE AP-S International Symposium on Antennas and Propagation*, Washington, USA, July 3–8, 2011.
23. Chew, W. C., *Waves and Fields in Inhomogeneous Media*, IEEE Press, New York, 1995.
24. Phaebua, K., C. Phongcharoenpanich, M. Krairiksh, and T. Lertwiriyaprapa, "Path-loss prediction of radio wave propagation in an orchard by using modified UTD method," *Progress In Electromagnetics Research*, Vol. 128, 347–363, 2012.
25. Rappaport, T. S., *Wireless Communications: Principles and Practice*, Prentice Hall, 2002.
26. Ndzi, D. L., M. A. M. Arif, A. Y. M. Shakaff, M. N. Ahmad, A. Harun, L. M. Kamarudin, A. Zakaria, M. F. Ramli, and M. S. Razalli, "Signal propagation analysis for low data rate wireless sensor network applications in sport grounds and on roads," *Progress In Electromagnetics Research*, Vol. 125, 1–19, 2012.
27. Bui, V. P., X. C. Wei, and E. P. Li, "An efficient simulation technology for characterizing the ultra-wide band signal propagation in a wireless body area network," *Journal of Electromagnetic Waves and Applications*, Vol. 24, Nos. 17–18, 2575–2588, 2010.